

# Complex light: Dynamic phase transitions of a light beam in a nonlinear non-local disordered medium

Claudio Conti\*

Research center “Enrico Fermi” Via Panisperna 85/A 00184, Rome, Italy and  
Reserch center SOFT INFM-CNR, University “La Sapienza,” P. A. Moro 2, 00185, Rome, Italy

(Dated: November 12, 2018)

The dynamics of several light filaments (spatial optical solitons) propagating in an optically nonlinear and non-local random medium is investigated using the paradigms of the physics of complexity. Cluster formation is interpreted as a dynamic phase transition. A connection with the random matrices approach for explaining the vibrational spectra of an ensemble of solitons is pointed out. General arguments based on a Brownian dynamics model are validated by the numerical simulation of a stochastic partial differential equation system. The results are also relevant for Bose condensed gases and plasma physics.

## I. INTRODUCTION

At low temperature, the dynamics of complex media is dominated by the potential energy landscape (PEL), i.e. the multi-dimensional surface of the potential energy as a function of the molecular coordinates. [1, 2, 3, 4] A disordered system sampling different PEL configurations undergoes “dynamic phase transitions,” perhaps one of the most spectacular ideas of the physics of complexity [5, 6, 7, 8]. For the dynamic glassy transition, observed in a certain class of (glass-forming) supercooled liquids, this “configurational sampling” is at the origin of an increase of viscosity of several orders of magnitudes, up to values comparable to solids (for recent reviews see for example [9, 10]). This phenomenon cannot be directly ascribed to a purely thermodynamic transition; conversely, it is now widely accepted as a dynamic effect. During cooling, different PEL regions are visited, and the almost abrupt change of viscosity is associated to the transition from “saddle-dominated” to “minima-dominated” PEL basins. Since phonons are the elementary excitations around minima of the PEL, this process is also denoted “phonon-saddle” transition, and can be realized while keeping fixed the temperature and acting on some parameter, like the particle density or the interaction range. [11]

It is not difficult to recognize the fundamental character of these ideas, and the fact that they are not limited to the specific contexts where they originally developed. In this article I will show that a light beam propagating in disordered medium (i.e. a medium with negligible optical losses whose refractive index is randomly varying) may undergo a sort of dynamic phase transition. This happens when, due to an optically nonlinear response, multiple filaments are generated. Their number and properties depend on the mutual interaction range and, in essence, they behaves like molecules in a complex

medium, exhibiting dynamic phases. The process can be described in terms of the appropriately defined “inherent structures” and “saddles,” in perfect analogy with the physics of disordered materials. This qualifies as a sort of *soft*, or *complex*, light.

Here the word “filament” (roughly) identifies a spatial soliton (SS), which is a non-diffracting light beam generated in an optically nonlinear medium, with an intensity dependent refractive index. [12, 13, 14] If a sufficiently intense laser light propagates in such a material, self-induced trapping counteracts the natural tendency to diffract, and a tightly focused SS can be observed. For example, in nematic liquid crystals (NLC), with laser wavelength in the near infrared, it is possible to generate very thin (few microns waist) SSs, able to propagate undistorted for millimeters: hundreds of times the distances attainable in absence of a nonlinear self-action. [15, 16, 17]

At each SS is associated an optically induced perturbation  $\Delta n$  to the refractive index, which is at the origin of the self-focusing. If the incident beam is sufficiently wide many SSs are generated by the same input, as shown for example in [16, 18, 19]. These filaments may propagate with various degrees of interaction, relying on the material properties and, in particular, on the so-called “non-locality”, which can be kept in mind as the ratio between the spatial extension of the refractive index perturbation induced by one filament and its transverse intensity waist. In NLC, the degree of nonlocality can be simply controlled by a voltage bias,[20] and hence the dynamic phase transition may be induced accordingly.[21]

The following results not only are well suited to describe light-soft-matter interaction (as in [16, 18, 20, 21, 22]), but can be applied to interpret the dynamics of ultrashort laser pulses propagating in air, [23, 24] as well solitons in photorefractives,[25, 26] media with thermal nonlinearities and plasmas, [27, 28, 29] semiconductors [30], discrete solitons (see for example [31] and references therein), plasmas [29] and Bose-condensed gases [32, 33].

This article is aimed to the introduction of the leading idea, and to a phenomenological description, supported by Brownian dynamics and stochastic partial differen-

---

\*Electronic address: claudio.conti@phys.uniroma1.it;  
URL: <http://nlo.phys.uniroma1.it>

tial equations (PDEs) numerical simulations. In order to simplify as much as possible the presentation no attempt will be made to a theoretical analysis, which is deferred to future publications. In section II the model for the propagation of several light filaments in a random medium is linked with Brownian dynamics. In section III evidences of phase transitions from numerical simulations are reported. Section IV is dedicated to the definition and the analysis of the so-called inherent structures. In section V the generalized inherent structures are considered for the final settlement of the dynamic phase transition. In section VI the noise quenching process is addressed. In section VII a connection with the theory of random matrices and the so-called dynamic structure factor is established. In section VIII numerical simulations of a well known model in nonlocal soliton theory validate the general arguments of the manuscript. Conclusions are drawn in section IX.

## II. REDUCTION TO A BROWNIAN DYNAMICS MODEL

For the sake of simplicity, the analysis is done with reference to one-dimensional (1+1D propagation) beams. Indeed, differently from standard thermodynamic transitions, dynamic transitions can be obtained in low dimensional systems. Additionally, the considered case reflects typical experimental geometries for the investigation of modulational instability (see e.g. [18, 19]). The generalization to higher dimensional problems of what follow can be readily imagined. Consider the Fock-Leontovich equation, which describes the paraxial optical propagation in a nonlinear medium:

$$2ik \frac{\partial A}{\partial z} + \frac{\partial^2 A}{\partial x^2} + 2k^2 \frac{\Delta n[I]}{n} A = 0. \quad (1)$$

$A(x, z)$  is the complex amplitude of the optical field such that  $I = |A(x, z)|^2$  is the intensity,  $k = 2\pi n/\lambda$  is the wave-vector and  $n$  the refractive index at wavelength  $\lambda$  in absence of non-linear effects.  $\Delta n$  is the optical induced perturbation to  $n$ , its functional relation with  $I$  is non-local: the specific distribution of  $\Delta n(x, z)$  depends on the whole profile  $I(x, z)$ . Various models are given in the literatures relating  $\Delta n$  and  $I$ , as the Kukhtarev equations for photorefractives, (for a review, see Del Re and coworkers in [13]) the heat equation for thermal nonlinearities, [28, 29] re-orientational equations for liquid crystals, [34] mode coupling theory for soft-matter, [22] or generic nonlocalities. [35, 36, 37, 38]

For relatively low intensities  $\Delta n$  is linear with  $I$  and, in the presence of many incoherent filaments, it can be written as the sum of the intensity distributions of the filaments, with  $p = 1, 2, \dots, N$ . The overall  $\Delta n$  is thus the sum of the index perturbations of each SS:

$$\Delta n[I] = \sum_{p=1}^N \Delta n[I_p]. \quad (2)$$

Eq. (2) is valid whenever  $\Delta n/n \ll 1$ , as typically verified in the reported experiments, and when the filaments are mutually incoherent, i.e. the relative phase between pairs of them is randomly varying. The latter hypothesis typically holds in soft-matter, by taking into account that the SSs spontaneously generate from noisy intensity perturbations, and propagate in a thermally fluctuating medium. Furthermore, in the presence of many filaments the effects of the relative phases and, more in general, of the specific form of  $\Delta n[I]$  can be negligible. This is analogous to the typical approach in statistical physics where, quite often, the particular profile of pair-interaction potentials can be replaced by some simple model like the Lennard-Jones potential. [39]

Following a perturbative analysis, the effect of the index perturbation due to all SSs on the trajectory of the generic filament  $p$  is considered. For  $N$  identical *stable* solitons with intensity bell-shaped profile  $I_S(x)$ ,  $\Delta n_S(x) = \Delta n[I_S](x)$ , and average position  $x_p(z)$ , using the Ehrenfest's theorem of standard quantum mechanics, applied to the Schrödinger-like Eq. (1), one has for the generic filament

$$m \frac{d^2 x_p}{dz^2} = - \int_{-\infty}^{\infty} I_S(x - x_p) \frac{\partial \Delta n/n}{\partial x} dx, \quad (3)$$

with  $m = \int I_S(x) dx$  the power (per unit length along the  $y$  direction) into each filament, which plays the role of the particle mass. The index perturbation is

$$\frac{\Delta n}{n} = \frac{1}{n} \sum_{q=1}^N \Delta n_S(x - x_q), \quad (4)$$

which used in (3) yields

$$\begin{aligned} m \frac{d^2 x_p}{dz^2} &= \\ & \sum_{q=1}^N \int_{-\infty}^{\infty} I_S(x - x_p) \frac{\partial \Delta n_S(x - x_q)/n}{\partial x} dx = \\ & - \sum_{q=1}^N \int_{-\infty}^{\infty} \frac{\partial I_S}{\partial x}(x - x_p) \frac{\Delta n_S(x - x_q)}{n} dx = \\ & \frac{\partial}{\partial x_p} \sum_{q=1}^N \int_{-\infty}^{\infty} I_S(x - x_p) \frac{\Delta n_S(x - x_q)}{n} dx = \\ & - \frac{\partial}{\partial x_p} \sum_{q=1}^N V(x_p - x_q) \end{aligned} \quad (5)$$

with

$$V(x) = - \frac{1}{n} \int_{-\infty}^{\infty} \Delta n_S(\xi + \frac{x}{2}) I_S(\xi - \frac{x}{2}) d\xi, \quad (6)$$

the pair-interaction potential. Many derivations of similar results can be found in the literature on solitons and

solitary waves (see e.g. [40, 41] and references therein). Here the analysis is specialized for the potential energy landscape interpretation.

In (5) the self-interaction term ( $p = q$ ) can be retained since it clearly gives a vanishing contribution. Finally

$$m \frac{d^2 x_p}{dz^2} = -\frac{\partial \Phi}{\partial x_p} \quad (7)$$

and  $\Phi = \Phi(x_1, x_2, \dots, x_N)$  is the overall potential energy surface (the PEL) given by the sum of pair-wise interaction terms:

$$\Phi = \frac{1}{2} \sum_{j=1}^N \sum_{k=1}^N V(x_j - x_k). \quad (8)$$

The dynamics along the direction of propagation is hence formally reduced to an ensemble of particles, evolving with “time”  $z$ . The fluctuations of the medium result into a random contribution to  $\Delta n$  that can be phenomenologically included in the model as a Langevin force  $\eta_p(z)$ :

$$m \frac{d^2 x_p}{dz^2} = -\frac{\partial \Phi}{\partial x_p} + \eta_p(z). \quad (9)$$

In the following, I will take for  $\eta_p$  a normally distributed white noise:

$$\langle \eta_p(z) \eta_q(z') \rangle = S_p^2 \delta_{pq} \delta(z - z') \quad (10)$$

with  $S_p^2$  the noise “power” and the brackets denoting a statistical average over disorder.  $\eta_p(z)$  takes into account the fluctuations of the refractive index and defines a realization of the random soft-medium.

Note that, in typical Langevin models, the random term is accompanied by a dissipative term, which is in general dependent on the lossy mechanisms in the medium, like viscosity. In the limit of small losses and small noise such a term can be neglected, as it will be done in the following in order to leave the treatment as general and simple as possible. The qualitative agreement with numerical results in section VIII, and experiments [21], supports this approach.

The explicit shapes of  $I_S$  and  $\Delta n_S$  are due to the particular nonlinear mechanism; for the present purpose a Gaussian ansatz for both of them is appropriate, since non-local optically nonlinear media are being considered. [34, 35, 37] Taking

$$\begin{aligned} I_S(x) &= I_0 \exp\left(-\frac{x^2}{2w^2}\right) \\ \Delta n_S(x) &= \Delta n_0 \exp\left(-\frac{x^2}{2v^2}\right) \end{aligned} \quad (11)$$

gives

$$V(x) = V_0 \left[ 1 - \exp\left(-\frac{x^2}{2u^2}\right) \right] \quad (12)$$

with  $V_0 = \Delta n_0 I_0 [2\pi v^2 w^2 / (v^2 + w^2)]^{1/2}$  and  $u^2 = v^2 + w^2$ .  $V(x)$  is a Gaussian function within an arbitrary additive constant. It is written as in (12) in order to have a vanishing  $\Phi$  when all the solitons are in the same position (“condensed phase”).  $u^2$  is the sum of the variances of  $I_S$  and  $\Delta n_S$  and provides a measure of the interaction range between the SSs for a fixed  $w$ , like  $u/w$  that will be used in the following. Each filament increases the refractive index (the medium is assumed to be focusing,  $\Delta n_0 > 0$ ) and the interaction is purely attractive, so that  $V_0 > 0$ .

The previous formulation points the connections with statistical physics while reducing the model to a system of interacting classical particles undergoing Brownian motion, a typical model for colloids, where the formation of clusters at the glass-transition is a well-known process (see e.g. [42, 43, 44]).

However, before proceeding, it is fruitful to point out a subtle issue associated to Eqs. (9) and (12). It is well expected that a finite number of classical particles, interacting by a purely attractive potential, will oscillate around the center of mass at equilibrium (i.e. for long times). This implies that only one energy minimum does exist and corresponds to the condensed phase. At a first glance, no dynamic phase transition, due to local minima of the PEL, is expected. Nevertheless, in the case under consideration, it is clearly not possible to consider an arbitrarily large propagation distance (corresponding to long times). If losses are negligible and if the maximum observation range (in  $z$ ) is limited by the spatial extension of the sample, damping mechanisms can be neglected and local PEL minima play a role.

### III. NUMERICAL SIMULATIONS OF THE BROWNIAN DYNAMICS MODEL

A typical distance between resolvable (by means of the observation of scattered light from the sample) spatial solitons, generated for example by modulational instability, can be taken as 6 times their waist  $w$ . Hence, considering thin solitons with waist  $w = 5\mu\text{m}$  and taking tens of filaments implies an input waist of the order of  $500\mu\text{m}$ , which is comparable to those typically employed in experiments (see e.g. [16, 18]). In the following two representative cases will be considered:  $N = 10$  and  $N = 30$  (the principal dynamic phase transition, considered below, is obtained up to the largest considered  $N = 100$ , not reported). In all the simulations the filaments are chosen uniformly distributed at  $z = 0$ , with mutual distance  $6w$ .

The noise “power” is measured by the corresponding adimensional quantity

$$\nu_p^2 = \frac{w}{V_0^{3/2} m^{1/2}} S_p^2, \quad (13)$$

which is taken independent from  $p$ , for the sake of simplicity:  $\nu_p^2 = \nu^2$ . The amount of noise to be included in the simulations clearly relies on the specific material

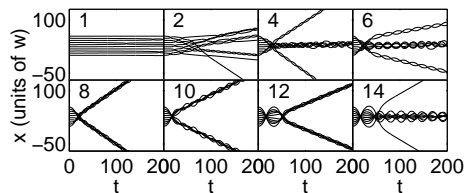


FIG. 1: Filaments trajectories Vs the normalized propagation coordinate  $t$  for a given noise realization and various values of the interaction range  $u/w$  (here  $N = 10$ ).

(in particular, on the thermal coefficient of the refractive index and on the sample temperature); however it is found that the numerical results are very robust with respect to noise, and very similar findings are obtained when  $\nu$  is varied by order of magnitudes. Hence only the case  $\nu = 0.001$  will be reported as a representative example. The stochastic ordinary differential equations (9) are solved by a second order scheme, whose accuracy has been thoroughly investigated and compared with other approaches.[45] The results have been validated by halving the integration step and doubling the number of realization in many cases.

As discussed above, a dynamic transition is attained while increasing the density, or equivalently the interaction length  $u/w$ . [11] Here, this corresponds to increase the degree of nonlocality. In figure 1, some realizations of the SSs trajectories, obtained by the numerical solution of Eqs. (9) when  $N = 10$ , are shown for various  $u/w$ . The adimensional “time”  $t = z/[w(V_0/m)^{1/2}]$  is used on the horizontal axis. For small  $u/w$  the filaments propagate in the presence of a reduced interaction. Conversely, while increasing  $u/w$ , various clusters are formed and their number and positions vary with each realization of the noise. A similar result is obtained in the case  $N = 30$  (fig. 2)

In figures 3 and 4, the “final” (i.e. at a fixed  $t = t_{max}$ ) position of each SS is shown Vs  $u/w$ , with the results for 10 noise realizations superimposed. Clearly, in certain ranges of the control parameter  $u/w$  the statistics of the final positions are highly peaked around 2 or 3 clusters, while they spread over a broad region in other ranges. The appearance of an interval for  $u/w$  where two dominant clusters are generated is evident. This is referred to as the “principal dynamics phase transition”. In the case  $N = 10$  a phase with 3 clusters is also present and it is somehow more noisy in the case for  $N = 30$ . For a very large  $u/w$  the nonlocality is such that all the SSs oscillate around an equilibrium position, this has been above indicated as the condensed phase.

Similar results are obtained for an odd number of filaments (e.g.  $N = 21$ ). In that case, in correspondence of the principal dynamic phase transition, an additional SS is found at the middle of the two clusters.

An open issue is the existence of fractal structures as those investigated in [46].

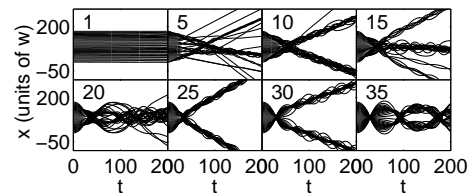


FIG. 2: Filaments trajectories Vs the normalized propagation coordinate  $t$  for a given noise realization and various values of the int

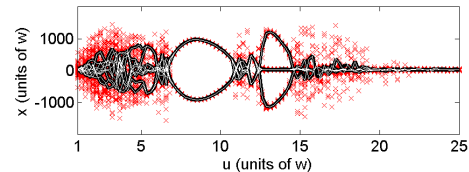


FIG. 3: (Color online) Crosses, filament positions at  $t_{max} = 1000$  for 10 noise realizations; thick black line, average position (see text); white line, inherent structures (here  $N = 10$ ).

#### IV. THE INHERENT STRUCTURE

Figures 3 and 4 also show the average filament positions Vs  $u/w$ , when  $N = 10$  and  $N = 30$  respectively. Note that the positions are determined at a very large  $t$  so that the clusters are “stabilized,” and that the average positions for each filament (thick black line in the figures) are shown superimposed (i.e. they are not the average positions among all the filaments), so that the thick black line provides a visualization of cluster distribution.

Disordered phases are alternated with others in which a fixed number of clusters is obtained. In order to address the existence of some kind of phase transition it is necessary to introduce a “control parameter”, as outlined in the mentioned literature. [8, 10] With this aim, I start pointing out the *inherent structure* (IS) associated to the numerical simulations. Once fixed a maximum value for the time  $t_{max}$ , the final distribution of filaments is used as guess for a conjugate gradient minimization procedure that finds the nearest minimum of the interaction potential  $\Phi$ . The corresponding vector of positions  $(x_1, x_2, \dots, x_N)$  is the IS. [2, 47] Its role is evident when superimposing the plots of the average final positions for the considered realizations (thick black line in Figs. 3 and 4) and those of the average IS (thin white line in Figs. 3 and 4). Clearly, the latter provide information on the number and the positions of the generated clusters.

According to the literature about complex media, [8, 10] the average potential energy  $e_{IS}$  of the IS is an appropriate control parameter for the dynamic phase-transition. In figures 5 and 6,  $e_{IS}$  (in units of  $V_0$ ) is plotted Vs  $u/w$ . The minimum for the potential energy is obtained at large  $u/w$  when all the solitons are in the same position and corresponds to  $\Phi = 0$  (condensed phase);

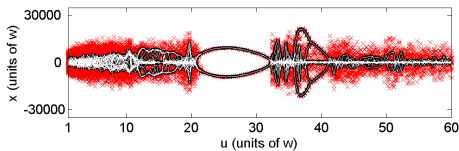


FIG. 4: (Color online) Crosses, filament positions at  $t_{max} = 6000$  for 10 noise realization; thick black line, average position (see text); white line, inherent structures (here  $N = 30$ ).

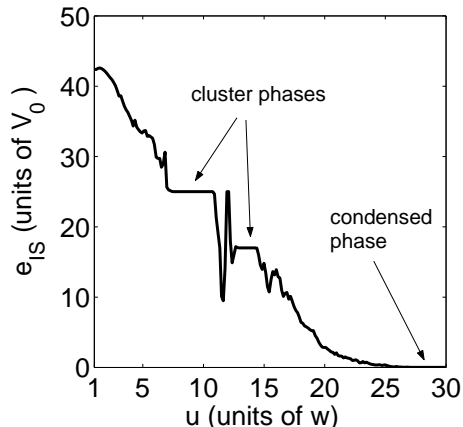


FIG. 5: Average potential energy  $\Phi$  of the inherent structure  $e_{IS}$  in units of  $V_0$  Vs  $u/w$ ; 1000 noise realizations have been considered ( $N = 10$ ).

conversely when the solitons are uniformly distributed (small  $u/w$ )  $\Phi$  is at maximum. Hence, while increasing  $u/w$ ,  $\Phi$  is reduced, due to the coagulation mechanism. The data in figures 5 and 6 show a decrease of  $e_{IS}$  Vs  $u/w$  up to the first plateau, at the formation of two clusters. The corresponding value of  $e_{IS}/V_0$  is obtained af-

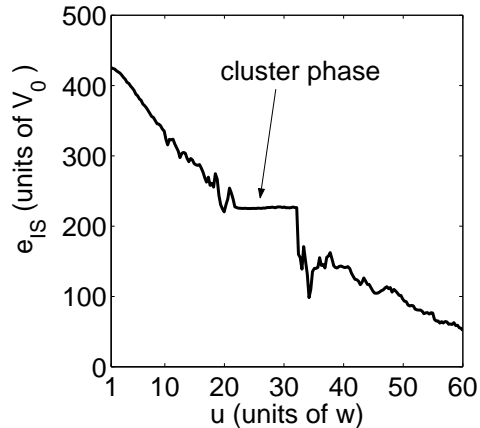


FIG. 6: Average potential energy  $\Phi$  of the inherent structure  $e_{IS}$  in units of  $V_0$  Vs  $u/w$ ; 100 noise realizations have been considered ( $N = 30$ ).

ter (8), by observing that, when two clusters of  $N/2$  SSs are formed (for  $N$  even),  $\Phi/V_0 \rightarrow N^2/4$  as their mutual distance goes to infinity. The plateau for  $N = 10$  corresponds to  $e_{IS}/V_0 = 25$ , and to  $e_{IS}/V_0 = 225$  for  $N = 30$ .

The trend is conserved for various numbers of filaments. The scale on the  $u/w$  axis changes with  $N$  (see Figs. 5 and 6) because the degree of nonlocality needed for the phase transition obviously increases with the number of filaments.

## V. THE GENERALIZED INHERENT STRUCTURE

For the definitive settlement of the phonon-saddle transition, the so-called *generalized inherent structure* (GIS) must also be taken into account. [6, 7, 48, 49] It is defined as the nearest stationary point of the PEL (where all the forces are zero) to the final configuration. The latter is used as a guess in a nonlinear solver (I used the c05pbf NAG routine, Mark 19) for the  $N$  equations  $\partial\Phi/\partial x_p = 0$ , whose solution, given by a vector  $(x_1, x_2, \dots, x_N)$  is just the GIS. The saddle-order  $K_{GIS}$  of the GIS is the number of the negative eigenvalues (imaginary frequencies) of the Hessian of  $\Phi$ , [see Eq. (14) below] calculated at the GIS; if  $K_{GIS} = 0$  the GIS is a minimum.

For any realization of the system there is one IS and one GIS. In a phonon-dominated phase the two structures are the same and  $K_{GIS} = 0$ . Conversely, in a saddle-dominated phase  $K_{GIS} > 0$ , but it tends approximately to zero (on average over many realizations) in correspondence of the dynamic phase-transition. [6, 7, 48, 49]

To understand the physical meaning of the GIS, consider the principal dynamic phase transition. While the IS corresponds to the filaments equally distributed between the two clusters, the GIS differs for some of the SSs positioned at intermediate places; it denotes the way the system may escape from the energy minimum. Clearly, if the noise-averaged  $K_{GIS}$  is high the probability to find a direction in PEL to get out from the local minimum of  $\Phi$  is high: it somehow measures the number of escape directions from the PEL minimum. Actually, the average  $K_{GIS}$  never reaches the zero as discussed in [49], because this would correspond to a complete freezing of the system.

Figure 7 shows the noise-averaged  $K_{GIS}$  Vs  $u/w$  when  $N = 10$ . It clearly reveals a saddle-phonon transition in proximity of  $u/w = 8$ ; consistently with the phase-diagram in figure 5. For larger values of  $u/w$ , the additional dynamic phase transitions are not well defined (i.e.  $K_{GIS}$  stays around one or two units) due to the limited number of particles. This also clarifies the reason for introducing a “principal” dynamic phase transition, as done above. The latter, in the considered numerical simulations, always corresponds to the formation of two clusters. This is confirmed in the case  $N = 30$  (shown in figure 8) where, due to an increased number of degrees of freedom, the transition is more evident, and happens, as

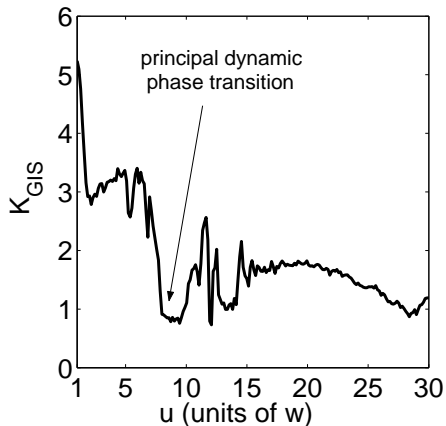


FIG. 7: Average saddle-order for the case  $N = 10$ , other parameters as in fig. 5.

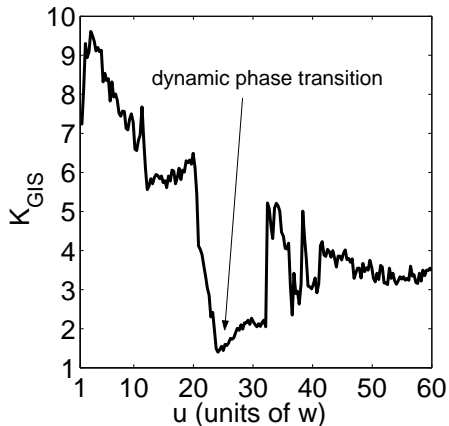


FIG. 8: Average saddle-order for the case  $N = 30$ , other parameters as in fig. 6.

before, when two clusters are generated. The transition becomes more evident as larger values of  $N$  are considered, and it is found up to the largest considered value (i.e.  $N = 100$ ). Nevertheless, the case  $N = 10$  shows evidence of this phenomenon, which is hence observable even with a limited number of filaments. Roughly speaking a given ensemble of filaments can self-organize in various way in order to form clusters. Two symmetrical clusters is obviously a strong “attractor” for the system, because there is only one way to organize it (conversely a larger number of clusters can be formed with different aggregations of solitons). This mechanism strongly resembles the cluster formation in coupled chaotic maps, a well known example of complex system. [50]

## VI. NOISE QUENCHING

The standard deviation  $\Delta e_{IS}$  of  $e_{IS}$  has a universal trend (with respect to number of filaments, their initial distance and the amount of noise), which is shown in figures 9 and 10. Moving towards a non-local region (i.e. increasing the interaction range  $u/w$ )  $\Delta e_{IS}$  grows (in the landscape dominated phase [10]) up to the dynamic phase-transition, where small values are again achieved (in the cluster phase). This quantity has the same trend of the corresponding one investigated, for example, in [51] in a Lennard-Jones material glass. Very similar results are obtained when simulating a larger number of filaments, and for various values of the noise power.

A reduction of the noise (“quenching”) in correspondence of the glassy-phase is hence evident. To confirm this effect, I show in figures 11 and 12, the relative maximum deviation from the average position. This quantity, denoted  $\varepsilon_x$  is calculated by taking the maximum deviation from the average (over the considered noise realizations) position  $\langle x \rangle$  for each filament (at  $t = t_{max}$ ), dividing by  $\langle x \rangle$  and then averaging the resulting quantity over all the  $N$  filaments. It measures the noise in the SS positions, and reproduces the same trend of  $\Delta e_{IS}$ . Before the phase transition all the SSs diffuse into a wide region, while after the phase transition they are locked inside each cluster.

In the experiments this phenomenon is resolved in time, while changing the control parameter for the non-locality (e.g. the voltage in NLC experiments [20]). This means that, since the medium is fluctuating, before the transition the number and the positions of the clusters are rapidly varying. Conversely, when the two clusters are formed, the intensity profile “slows down”, and the noise is quenched; this resembles the “critical slowing down” [9] in glassy material system (see also the section VIII and the movie cited below).

## VII. VIBRATIONAL SPECTRA AND THE RANDOM MATRICES

A variety of issues spontaneously rises, once some analogy with a disordered medium has been ascertained. In particular, those concerning the spectrum of the fluctuations and ultimately the propagation of “sound-waves” (or better “displacement-waves”). These are associated to the vibrational spectra of the ensemble of solitons.

The analysis of sound-waves is one of the most important issues in the physics of glassy systems (see for example [52] and references therein). According to some authors, the appearance of ultra-high frequency sound can be related to the vibrational spectrum of the material and, in particular, and to an excess of states denoted “boson peak” (see [11] and references therein). The transposition of these ideas to nonlinear optical propagation is beyond the scope of this article. However, it is interesting to observe that one of the most successful theories of

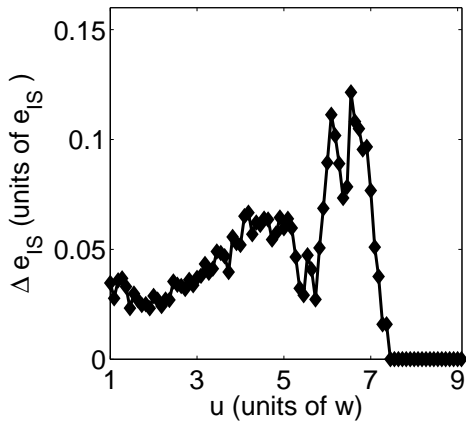


FIG. 9: Standard deviation of the energy of the inherent structures for 100 noise realizations Vs  $u/w$  ( $N = 10$ ,  $t_{max} = 1000$ ).

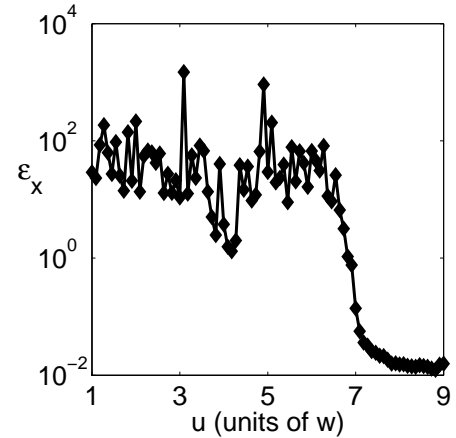


FIG. 11: Maximum relative deviation from the average position, averaged over all the  $N = 10$  filaments Vs  $u/w$ . Parameters as in fig. 9.

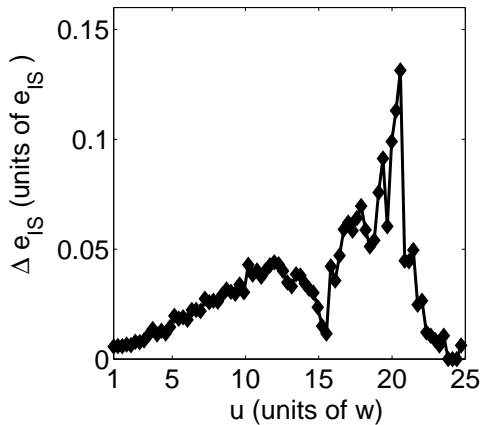


FIG. 10: Standard deviation of the energy of the inherent structures for 100 noise realizations Vs  $u/w$  ( $N = 30$ ,  $t_{max} = 6000$ ).

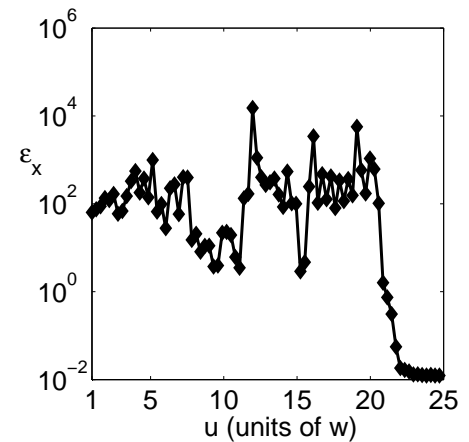


FIG. 12: Maximum relative deviation from the average position, averaged over all the  $N = 30$  filaments Vs  $u/w$ . Parameters as in fig. 10.

structural glasses, the random-matrices approach, [8, 53] also seems well suited to describe the vibrational spectra of the positions of a number of optical spatial solitons in a disordered medium.

Given some configuration of the filaments  $(x_1, x_2, \dots, x_N)$ , which can be either the instantaneous distribution at  $t_{max}$ , or the IS, [11] the vibrational spectra can be found as the eigenvalues of the Hessian matrix  $H_{pq}$  ( $p, q = 1 \dots N$ ):

$$H_{pq} = \frac{\partial^2 \Phi}{\partial x_p \partial x_q} = \delta_{pq} \sum_{k=1}^N V''(x_p - x_k) - V''(x_p - x_q), \quad (14)$$

with  $V'' \equiv d^2V/dx^2$ . Due to noise (and eventually to chaos), the considered configuration has a certain statistical distribution; the problem is hence reduced to find

the corresponding statistical distribution of the eigenvalues of  $H_{pq}$ . Various approaches have been developed and successfully applied to explain some material glass features. [8, 53] What follows suggests that the random matrices approach could be very fruitful even in this field of research.

Consider an experiment in which the position of each SS can be retrieved by the scattered light from the top of the sample (as those in the mentioned literature on *nematicons* [15, 16]); the resulting images appear as a number of superimposed light filaments, each with its own few-microns waist, with overall intensity distribution  $I(x, z)$ . If a soliton profile  $I_S$  is associated to each SS, as discussed above,  $I(x, z)$  can be interpreted as a coarse-grained density of particles evolving along  $z$ . The squared modulus of the double-Fourier transform of the image  $I(x, z)$ , denoted  $S(k_x, k_z)$  (averaged over a given

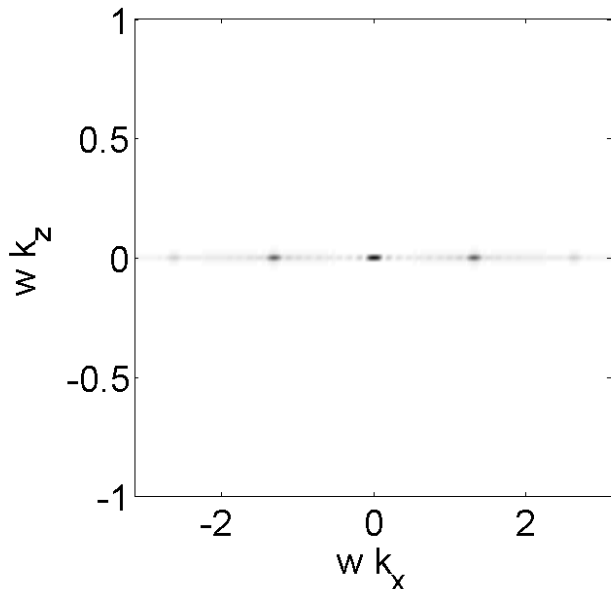


FIG. 13: Pseudo-color plot of the squared modulus of the Fourier transform of the course grained density (overall intensity profile) when  $N = 10$ ,  $u/w = 1$  and  $t_{max} = 200$ , averaged over 100 noise realizations.

number of noise realizations) can be interpreted as the so-called “dynamic structure factor” [39] of the soft-medium realized by the SSS, which play the role of interacting Brownian molecules.  $S(k_x, k_z)$  gives the frequency content in  $k_z$  of the  $z$ -evolution of the spatial “mode” at  $k_x$ . In other words, once fixed  $k_x$ ,  $S(k_x, k_z)$  provides information on the dynamics of each intensity perturbation with period  $2\pi/k_x$ . [56]

Consider, for example, the case in which all the solitons travel approximately parallel, with a reduced interaction. In this case, if  $\Delta x$  is the average mutual distance,  $S(k_x, k_z)$  is expected to be approximately given by a series of peaks around  $k_x = 2\pi m/\Delta x$  and  $k_z = 0$ , with  $m = 0, 1, 2, \dots$ . That is the  $k_z$ -bandwidth of each “mode” at  $k_x$  is very small. This happens, for example in the case  $N = 10$ , when  $u/w = 1$ , as shown in the inset in figure 1. Taking the corresponding numerical solution of eqs. (9), associating to each trajectory a soliton profile (a Gaussian profile in units such that  $w = 1$ ), evaluating the squared modulus of the Fourier transform of the resulting  $I(x, z)$ , and finally averaging over a given number of noise realizations, Fig. 13 is obtained, which appears as anticipated.

The aim of the random matrices approach is to predict the shape of  $S(k_x, k_z)$  with respect to some control parameter. In particular, under very general hypotheses, it has been shown that, when the interaction range grows (or equivalently the density of the particles is increased),  $S(k_x, k_z)$  develops a Brillouin peak with position that is linearly dependent on  $k_x$ . [53] This corresponds to an X-shape in the two dimensional level-plot of  $S(k_x, k_z)$ .

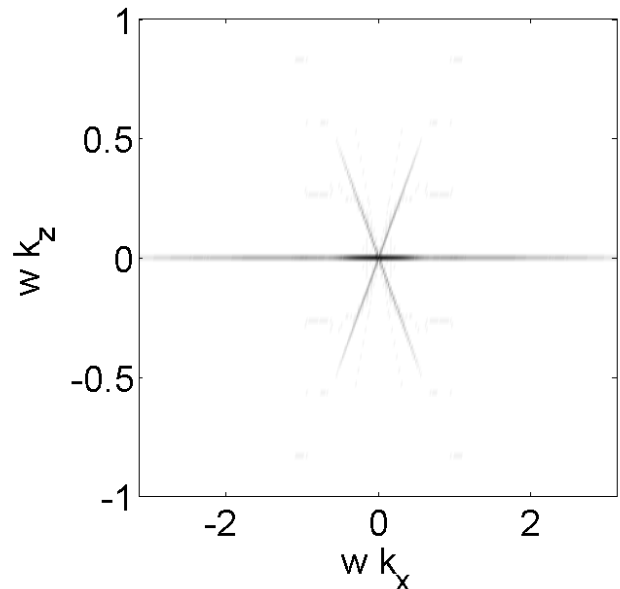


FIG. 14: Pseudo-color plot of the squared modulus of the Fourier transform of the course grained density (overall intensity profile) when  $N = 10$ ,  $u/w = 8$  and  $t_{max} = 200$ , averaged over 100 noise realizations.

Repeating the analysis of figure 13, for  $u/w$  at the dynamic phase transition, should provide some evidence of the predicted X-shape. This is exactly what happens, as shown in figure 14.

The formation of a Brillouin peak is obviously related to the geometry of the filaments distribution. However, it can be also associated to a movement of energy (or equivalently of “mass”, which corresponds to the beam power into each filament, as discussed above). Indeed, when two clusters are formed and move far apart each other, there is an evident energy transfer along  $x$ . In some sense the cluster movement is related to some wave-packet motion, in perfect analogy with sound waves in disordered media.

## VIII. NUMERICAL SIMULATIONS OF A STOCHASTIC PDE MODEL

In this section I consider a specific example in order to validate the previous arguments. Some numerical simulations of a stochastic PDE system (which is well known in the deterministic limit and has been successfully compared with experiments) are reported and reproduce the features previously described by the Brownian dynamics approach. For the sake of clearness and compactness, I will show sample results for nonlocalities up to the first dynamic transition (i.e. the formation of two dominant clusters). Additional data will be reported elsewhere.

The model equations are those of the so-called 1+1D exponential non-locality, which well describes solitons in



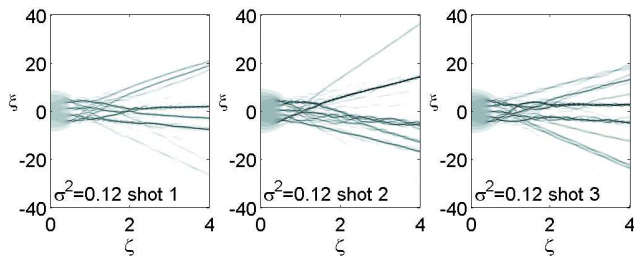


FIG. 15: Three realizations of the numerical solution of the stochastic PDE (15) for  $\sigma^2 = 0.12$ .

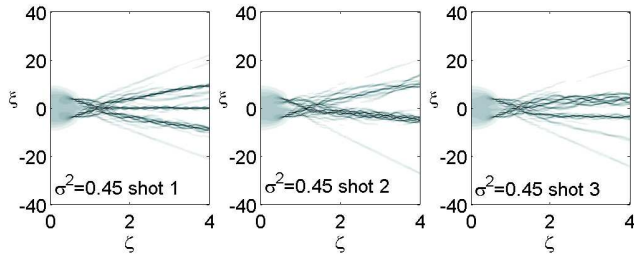


FIG. 16: Three realizations of the numerical solution of the stochastic PDE (15) for  $\sigma^2 = 0.45$ .

liquid crystals [18, 34], as well as thermal nonlinearities and plasmas [28, 29], and has been thoroughly studied (in absence of noise) in the literature (see e.g. [37, 38] and references therein). Using adimensional variables the PDE system (corresponding to Eq. (1)) reads as

$$\begin{aligned} i\partial_\zeta\psi + \partial_{\xi\xi}\psi + \rho\psi &= 0 \\ -\sigma^2\partial_{\xi\xi}\rho + \rho &= |\psi|^2 + A\eta(\xi, \zeta). \end{aligned} \quad (15)$$

In (15)  $\xi$  is the normalized transverse coordinate,  $\zeta$  is the normalized propagation distance,  $\psi$  is a complex field, corresponding to the electromagnetic field;  $\rho$  is the medium disturbance, which can be the director angle of NLC, or the temperature, or the density of the medium, depending on the specific physical system; its fluctuations are taken into account by a Langevin term, which is a white Gaussian stochastic process, such that  $\langle \eta(\xi, \zeta)\eta(\xi', \zeta') \rangle = \delta(\xi - \xi')\delta(\zeta - \zeta')$ , and  $A$  measures the amount of noise.  $\sigma^2$  is taken into account the nonlocality; as  $\sigma^2 = 0$ , the model reduces to the local integrable nonlinear Schrödinger equation; the degree of nonlocality increases with as  $\sigma^2$ . Equations (15) are solved by a pseudospectral approach (see e.g. [54]), which maps (15), via discrete Fourier transform, into coupled stochastic ordinary equations, which are then solved by the Heun algorithm. [55]

In figures 15,16 and 17 I show some realizations obtained with different values of the nonlocality parameters  $\sigma^2$ . The input profile is taken to be a super-Gaussian:

$$\psi(\xi, 0) = \exp(-(\xi/10)^4), \quad (16)$$

such that it corresponds to a flat intensity profile, on which various solitons are generated via modulational in-

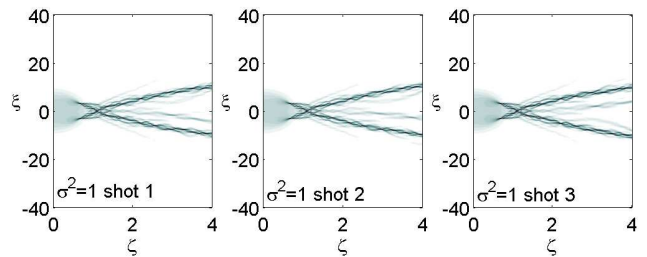


FIG. 17: Three realizations of the numerical solution of the stochastic PDE (15) for  $\sigma^2 = 1$ .

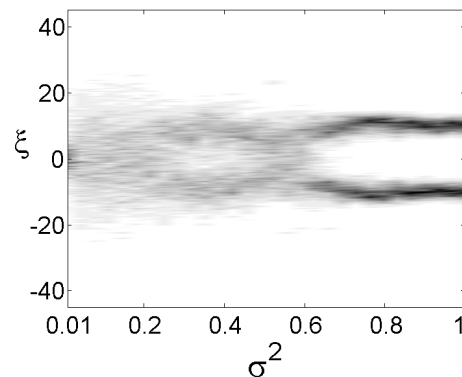


FIG. 18: Average intensity distribution at  $\zeta = 4$  over 100 noise realizations as a function of  $\xi$  and  $\sigma^2$ .

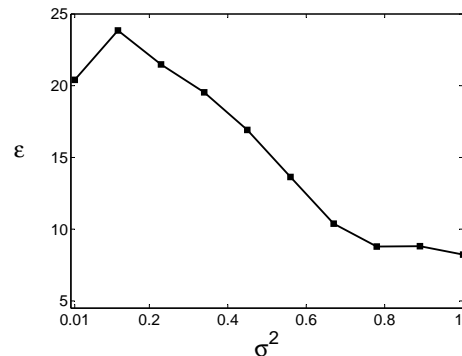


FIG. 19: Maximum relative deviation from the average profile versus the nonlocality parameter calculated at  $\zeta = 4$ .

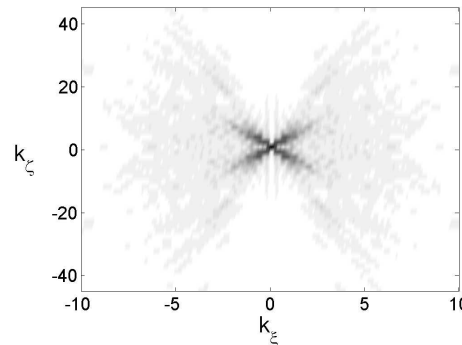


FIG. 20: Two dimensional Fourier transform of the intensity profile, average over 100 realization, when  $\sigma^2 = 1$ .

stability and interact while propagating along the  $\zeta$  direction. (The reported results correspond to  $A = 10^{-3}$ ).

Consistently with the analysis reported above, for small nonlocality various solitons are generated and travel almost independently, while at higher nonlocality clusters are formed, and two dominant aggregates of solitons are clearly evident when  $\sigma^2 = 1$ .

In figure 18 I show the intensity profile at  $\zeta = 4$  averaged over 100 realizations, it clearly reproduces the features in figures 3 and 4, where two dominant clusters appear at a threshold value of nonlocality.

Note from figs. 15-17 that, for small  $\sigma^2$ , the various shots are very different from each other, while at high nonlocality the two clusters distribution is “frozen.” [57]

The noise quenching mechanism is quantified in figure 19, where I show the noise figure  $\varepsilon = \varepsilon(\zeta = 4)$ , determined as

$$\varepsilon(\zeta) = \langle \max_{\xi} \left( \frac{|\psi(\xi, \zeta)|^2}{\langle |\psi(\xi, \zeta)|^2 \rangle} - 1 \right) \rangle, \quad (17)$$

and corresponding to the maximum (along the  $\xi$  direction) relative intensity deviation with respect to the average profile at  $\zeta = 4$ . Figure 19 shows a drastic reduction of noise at high nonlocality, in correspondence of the two clusters.

Finally, the vibrational spectrum (as described in the previous section) is calculated: the intensity distribution  $|\psi(\xi, \zeta)|^2$ , for a fixed  $\sigma^2$ , is Fourier transformed and averaged over the considered 100 realizations. The result for  $\sigma^2 = 1$  is shown in figure 20 and clearly displays the X-shape, addressed above. A similar picture is obtained for other values of nonlocality in correspondence of the two clusters formation.

## IX. CONCLUSION

The basic aim of this manuscript is to point out one of the possible connections between the physics of complex

media and that of intense laser light interacting with matter. During nonlinear optical phenomena in disordered media (or even in media where the disorder is induced by the input laser beam), the behavior of light can be interpreted using the same paradigms of modern statistical physics.

If a light filament, or spatial optical soliton, can be treated as a classical particle, many interacting spatial solitons correspond to a liquid or high density gas. If some noise is present in the system, a Brownian dynamics model is readily introduced, and the filaments behave like particles dispersed into a solvent, which is one of the simplest definitions of soft-matter. The dynamic phase transition is the natural way to describe phenomenological transformations, like the formation of clusters. This has been shown by numerical experiments in this article and experimentally in future publications.

Nonlinear optics can be hence used to test, theoretically and experimentally, some of the ideas of the physics of complexity, as well as the latter can be used to explain many high-field phenomena, like laser-filaments generation and interaction. In this manuscript these ideas have been applied to explain a possible manifestation of complex light.

## Acknowledgments

It is my pleasure to thank L. Angelani, B. Crosignani, E. Del Re, G. Ruocco, F. Sciortino and S. Trillo for their interest and for many stimulating discussions. A particular acknowledgement goes to M. Peccianti and G. Assanto, who made possible the experimental investigation of dynamic phase transitions of light, as well as a very prolific research period for the author.

- 
- [1] M. Goldstein, *J. Chem. Phys.* **51**, 3728 (1969).  
 [2] F. H. Stillinger and T. A. Weber, *Phys. Rev. A* **25**, 978 (1982).  
 [3] H. Jonsson and H. C. Andersen, *Phys. Rev. Lett.* **60**, 2295 (1988).  
 [4] S. Sastry, P. G. De Benedetti, and F. H. Stillinger, *Nature* **393**, 554 (1998).  
 [5] K. K. Bhattacharya, K. Broderix, R. Kree, and A. Zippelius, *Europhys. Lett.* **47**, 449 (1999).  
 [6] L. Angelani, R. Di Leonardo, G. Ruocco, A. Scala, and F. Sciortino, *Phys. Rev. Lett.* **85**, 5356 (2000).  
 [7] K. Broderix, K. K. Bhattacharya, A. Cavagna, A. Zippelius, and I. Giardina, *Phys. Rev. Lett.* **85**, 5360 (2000).  
 [8] T. S. Grigera, V. Martin-Mayor, G. Parisi, and P. Verrocchio, *Nature* **422**, 289 (2003).  
 [9] Various authors in the special issue of *Physica (Amsterdam)* D, **107D**, Issue 2-4 (1997).  
 [10] P. G. De Benedetti and F. H. Stillinger, *Nature* **410**, 259 (2001).  
 [11] G. Parisi, *J. Phys.: Condens. Matter* **15**, S765 (2003).  
 [12] A. D. Boardman and A. P. Sukhorukov, eds., *Soliton Driven Photonics* (Kluwer Academic Publ., Dordrecht, 2001).  
 [13] S. Trillo and W. Torruellas, eds., *Spatial solitons* (Springer-Verlag, Berlin, 2001).  
 [14] Y. S. Kivshar and G. P. Agrawal, *Optical solitons* (Academic Press, New York, 2003).  
 [15] G. Assanto, M. Peccianti, and C. Conti, *Optics and Photonics News* **14**, 45 (2003).  
 [16] M. Peccianti, C. Conti, G. Assanto, A. De Luca, and C. Umetsu, *Nature* **432**, 733 (2004).  
 [17] X. Hutsebaut, C. Cambournac, M. Haelterman, J. Beeck-

- man, and K. Neyts, *J. Opt. Soc. Am. B* **22**, 1424 (2005).
- [18] M. Peccianti, C. Conti, and G. Assanto, *Phys. Rev. E* **68**, 025602(R) (2003).
- [19] M. Peccianti, C. Conti, and G. Assanto, *Opt. Lett.* **28**, 2231 (2003).
- [20] M. Peccianti, C. Conti, and G. Assanto, *Opt. Lett.* **30**, 415 (2005).
- [21] C. Conti, M. Peccianti, and G. Assanto, *Phys. Rev. Lett.* (2005), submitted.
- [22] C. Conti, G. Ruocco, and S. Trillo, *Phys. Rev. Lett.* **95**, 183902 (2005), arXiv:physics/0510172.
- [23] S. Skupin, L. Berge, U. Peschel, F. Lederer, G. Mejean, J. Yu, J. Kasparian, E. Salmon, J. P. Wolf, M. Rodriguez, et al., *Phys. Rev. E* **70**, 046602 (2004).
- [24] M. Rodriguez, R. Bourayou, G. Mejean, J. Kasparian, J. Yu, E. Salmon, A. Scholz, B. Stecklum, J. Eisloffel, U. Laux, et al., *Phys. Rev. E* **69**, 036607 (2004).
- [25] M. Segev, B. Crosignani, A. Yariv, and B. Fischer, *Phys. Rev. Lett.* **68**, 923 (1992).
- [26] Z. Chen, S. M. Sears, H. Martin, D. N. Christodoulides, and M. Segev, *PNAS* **99**, 5223 (2002).
- [27] F. Henninot, M. Debailleul, and M. Warenaughem, *Mol. Cryst. Liq. Cryst.* **375**, 631 (2002).
- [28] A. I. Yakimenko, Y. A. Zaliznyak, and Y. Kivshar, arXiv:nlin.PS/0411024v2 (2004).
- [29] A. G. Litvak, V. A. Mironov, G. M. Fraiman, and A. D. Yunakovskii, *Sov. J. Plasma Phys.* **1**, 31 (1975).
- [30] E. A. Ultanir, D. Michaelis, F. Lederer, and G. I. Stegeman, *Opt. Lett.* p. 251 (2003).
- [31] J. W. Fleischer, M. Segev, N. K. Efremidis, and D. N. Christodoulides, *Nature* **422**, 147 (2003).
- [32] L. Khaykovich, F. Schreck, G. Ferrari, T. Bourdel, J. Cubizolles, L. D. Carr, Y. Castin, and C. Salomon, *Science* **296**, 1290 (2002).
- [33] K. E. Strecker, G. B. Partridge, A. G. Truscott, and R. G. Hulet, *Nature* **417**, 150 (2002).
- [34] C. Conti, M. Peccianti, and G. Assanto, *Phys. Rev. Lett.* **91**, 073901 (2003).
- [35] A. W. Snyder and D. J. Mitchell, *Science* **276**, 1538 (1997).
- [36] V. M. Perez-Garcia, V. V. Konotop, and J. J. Garcia-Ripoll, *Phys. Rev. E* **62**, 4300 (2000).
- [37] O. Bang, W. Krolikowski, J. Wyller, and J. J. Rasmussen, *Phys. Rev. E* **66**, 046619 (2002).
- [38] W. Krolikowski, O. Bang, N. I. Nikolov, D. Neshev, J. Wyller, J. J. Rasmussen, and D. Edmundson, *J. Opt. B: Quantum Semiclass. Opt.* **6**, S288 (2004).
- [39] J.-P. Hansen and I. R. McDonald, *Theory of simple liquids* (Academic Press, London, UK, 1986), 2nd ed.
- [40] V. Perez-Garcia and V. Vekslerchik, *Phys. Rev. E* **67**, 061804 (2003).
- [41] L.-C. Crasovan, Y. V. Kartashov, D. Mihalache, L. Torner, Y. Kivshar, and V. M. Perez-Garcia, *Phys. Rev. E* **67**, 046610 (2003).
- [42] C. Donati, S. C. Glotzer, P. H. Poole, W. Kob, and S. J. Plimpton, *Phys. Rev. E* **60**, 3107 (1999).
- [43] C. N. Likos, *Physics Reports* **348**, 267 (2001).
- [44] E. R. Weeks and D. A. Weitz, *Phys. Rev. Lett.* **89**, 095704 (2002).
- [45] J. Qiang and S. Habib, *Phys. Rev. E* **62**, 7430 (2000).
- [46] S. V. Dmitriev, Y. S. Kivshar, and T. Shigenari, *Physica B* **316**, 139 (2002).
- [47] F. H. Stillinger and T. A. Weber, *Phys. Rev. A* **28**, 2408 (1983).
- [48] A. Cavagna, *Europhysics Letters* **53**, 490 (2001).
- [49] G. Parisi, arXiv:cond-mat/0301282 (2003).
- [50] K. Kaneko and I. Tsuda, *Complex Systems: Chaos and Beyond* (Springer-Verlag, Berlin, 2000).
- [51] F. Sciortino, W. Kob, and P. Tartaglia, *Phys. Rev. Lett.* **83**, 3214 (1999).
- [52] T. Scopigno, R. Di Leonardo, G. Ruocco, A. Q. R. Baron, S. Tsutsui, F. Bossard, and S. N. Yannopoulos, *Phys. Rev. Lett.* **92**, 025503 (2004).
- [53] T. S. Grigera, V. Martin-Mayor, G. Parisi, and P. Verrocchio, *Phys. Rev. Lett.* **87**, 085502 (2001).
- [54] J. P. Boyd, *Chebyshev and Fourier Spectral Methods* (Dover, New York, 2001), 2nd ed.
- [55] A. Greiner, W. Strittmatter, and J. Honerkamp, *J. Stat. Phys.* **51**, 95 (1988).
- [56] This is rigorously true only after the transient (along  $z$ ) during which the clusters are formed. However in the following the overall dynamics from  $t = 0$  is considered, for simplicity sake. I have checked that no substantial differences arise in the spectrum if the transient is removed before making the Fourier transform of  $I(x, z)$ .
- [57] A movie reporting various noise realizations for different  $\sigma^2$  can be downloaded at <http://nlo.phys.uniroma1.it/complexity.htm>